Extended State Observer Based Stator Flux Linkage Estimation of Nonlinear Synchronous Machines

Seunghun Jang[1], Bernd Pfeifer[1], Christoph M. Hackl[1], and Kyunghwan Choi[1]

[1]Affiliation not available

April 18, 2024

Extended State Observer Based Stator Flux Linkage Estimation of Nonlinear Synchronous Machines

1st Seunghun Jang
School of Mechanical Engineering
Gwangju Institute of Science and Technology
Gwangju, Republic of Korea
shjang7071@gm.gist.ac.kr

2nd Bernd Pfeifer
Laboratory for Mechatronic and Renewable Energy Systems (LMRES)
HM Munich University of Applied Sciences
bernd.pfeifer@hm.edu

3rd Christoph M. Hackl
Laboratory for Mechatronic and Renewable Energy Systems (LMRES)
HM Munich University of Applied Sciences
christoph.hackl@hm.edu

4st Kyunghwan Choi
School of Mechanical Engineering
Gwangju Institute of Science and Technology
Gwangju, Republic of Korea
khchoi@gm.gist.ac.kr

***Abstract*—Synchronous machines (SMs) are characterized as nonlinear dynamic systems, with stator flux linkages being critical for controller design. Among the developed methods for flux linkage estimation, the disturbance observer-based flux linkage estimator (DOB-FLE) is recognized as the state-of-the-art. However, DOB-FLE faces challenges in ensuring exponential convergence during transient states. To address this, this paper introduces an extended state observer-based flux linkage estimator (ESO-FLE), which represents an advancement over DOB-FLE. This novel approach utilizes extended states to model the nonlinear disturbance term as time-varying ramp signals, offering a contrast to the constant assumption employed in DOB-FLE. It concurrently estimates both the extended states and the flux linkages through an ESO. Simulation results from a 35-kW SM drive demonstrate that ESO-FLE provides superior transient performance under dynamic conditions compared to DOB-FLE.**

***Index Terms*—Extended state observer, disturbance observer, nonlinear synchronous machines, stator flux linkage, transient performance**

I. INTRODUCTION

Synchronous machines (SMs) are described as nonlinear dynamic systems with stator flux linkages. Accurate information on the stator flux linkages is required to design high-performance controllers for SM drives. For instance, differential and secant inductance information is used to design current controllers [1] and optimal reference generators [2], respectively. The flux linkage information itself can be utilized to predict the future behavior of the SM for model predictive control (MPC) [3].

The stator flux linkage maps can be obtained offline through identification experiments conducted across the entire operating range [6]. However, this offline identification cannot deal with real-time parameter changes in SMs caused by aging or abnormal operations, such as temperature rise or demagnetization.

Several studies present online estimation methods for the stator flux linkages. The stator flux linkages can be easily calculated by integrating the flux linkage dynamics defined in the α-β frame, but the integration results include integration errors. In [7], a high-pass filter was applied after the integration to remove the integration errors. This method was simple and did not use any SM parameter information, but the filter distorted the frequency response, particularly in the low-frequency region. Another simple online estimation method is to adopt the steady-state assumption for the flux linkage dynamics defined in the rotating d-q frame and to calculate the flux linkages directly from the steady-state model [9], [10]. The high-frequency current injection has recently been adopted for the stator flux linkage estimation [11] and has shown satisfactory steady-state performance. However, these approaches could not guarantee sufficient transient performance. Using a state observer, such as sliding mode observer [12] are extended Kalman filter [13], was proposed for online flux linkage estimation, but these observers were designed based on prior knowledge of machines parameters, which is difficult to obtain without accurate knowledge of the stator flux linkages.

Recently, online flux linkage estimators have been proposed, which do not require accurate knowledge of machine parameters but provide remarkable estimation performance. In [14], a disturbance observer-based flux linkage estimator (DOB-FLE) was proposed, which could estimate the flux linkages without knowing the accurate value of the inductance matrix, with the help of the DOB compensating for the nonlinear disturbance term. An advanced α-β frame-based estimator was presented in [15], where integration errors were estimated by a linear state observer and compensated for in the time domain, which differed from using a frequency-domain approach. Both methods presented in [14] and [15] offered remarkable estimation performance even using inaccurate nominal machine

This work was supported by Electronics and Telecommunications Research Institute (ETRI) grant funded by the Korean government. [24ZD1160, Regional Industry ICT Convergence Technology Advancement and Support Project in Daegu-GyeongBuk (Mobility)].

parameters. However, they struggled with ensuring exponential convergence during transient states, and their transient performance deteriorated when using a nominal parameter that differs greatly from the true parameter.

With this background, this paper presents an extended state observer-based flux linkage estimator (ESO-FLE), an advancement over DOB-FLE with improved transient performance. The key difference between the proposed ESO-FLE and DOB-FLE is that ESO-FLE introduces extended states to model the nonlinear disturbance term as time-varying ramp signals, in contrast to the constant assumption used in DOB-FLE. By doing so, both flux linkages and extended states can be estimated more accurately via an ESO. The effectiveness of the proposed ESO-FLE is numerically validated using a 35-kW interior permanent magnet synchronous machine (IPMSM).

II. Preliminaries

A. Nonlinear Synchronous Machine Model

The nonlinear flux linkage dynamics [16] are given by The SM is modeled in the rotating d-q frame as follows:

$$\dot{\boldsymbol{\lambda}}_{dq}(t) = \boldsymbol{v}_{dq}(t) - R_s \boldsymbol{i}_{dq}(t) - \omega_r \boldsymbol{J} \boldsymbol{\lambda}_{dq}(t), \tag{1}$$

with $\boldsymbol{z}_{dq} := \begin{bmatrix} z_d & z_q \end{bmatrix}^T$, $z = \lambda, v, i$, stator flux linkages $\boldsymbol{\lambda}_{dq}$, stator voltages $\boldsymbol{v}_{dq}$, stator currents $\boldsymbol{i}_{dq}$, stator winding resistance R_s, rotation matrix $\boldsymbol{J} := \begin{bmatrix} 0 & -1 \\ 1 & 0 \end{bmatrix}$, and electrical rotor speed w_r. The nonlinear flux linkages are generally modeled by a nonlinear function of the stator currents as $\boldsymbol{\lambda}_{dq}(t) = \boldsymbol{f}(\boldsymbol{i}_{dq}(t))$.

The followings are assumed:

- The stator winding resistance R_s is accurately known.
- The inverter nonlinearity and iron loss in the eletrical dynamics are neglected.
- The electrical rotor speed w_r varies slowly compared to electrical quantities.

B. Disturbance Observer-Based Stator Flux Linkage Estimator (DOB-FLE)

DOB-FLE, presented in [14], is based on the idea of seperating the nonlinear flux linkages into a linear term $\boldsymbol{L}_{s,0}\boldsymbol{i}_{dq}$ and a nonlinear disturbance term $\Delta_{\boldsymbol{\lambda}_{dq}}$ as follows:

$$\boldsymbol{\lambda}_{dq}(t) = \boldsymbol{L}_{s,0} \boldsymbol{i}_{dq}(t) + \Delta_{\boldsymbol{\lambda}_{dq}}(t), \tag{2}$$

which can be rearranged by

$$\boldsymbol{i}_{dq}(t) = {\boldsymbol{L}_{s,0}}^{-1} \left(\boldsymbol{\lambda}_{dq}(t) - \Delta_{\boldsymbol{\lambda}_{dq}}(t) \right), \tag{3}$$

where $\boldsymbol{L}_{s,0}$ denotes a constant nominal inductance matrix.

The following state-space model is obtained by substituting (3) into the nonlinear flux linkage dynamics (1):

$$\begin{cases} \dot{\boldsymbol{\lambda}}_{dq}(t) = \boldsymbol{v}_{dq}(t) - R_s {\boldsymbol{L}_{s,0}}^{-1} \left(\boldsymbol{\lambda}_{dq}(t) - \Delta_{\boldsymbol{\lambda}_{dq}}(t) \right) \\ \qquad\qquad - \omega_r \boldsymbol{J} \boldsymbol{\lambda}_{dq}(t) \\ \dot{\Delta}_{\boldsymbol{\lambda}_{dq}}(t) = 0 \\ \boldsymbol{i}_{dq}(t) = {\boldsymbol{L}_{s,0}}^{-1} \left(\boldsymbol{\lambda}_{dq}(t) - \Delta_{\boldsymbol{\lambda}_{dq}}(t) \right), \end{cases} \tag{4}$$

With $\dot{\boldsymbol{\lambda}}_{dq}$ and $\dot{\Delta}_{\boldsymbol{\lambda}_{dq}}$ as states, $\boldsymbol{v}_{dq}$ as inputs, and $\boldsymbol{i}_{dq}$ outputs, this model was shown in [14] to be observable; The linear state observer was designed in [14] to estimate the full states asymptotically and exponentially.

However, this model assumes $\dot{\Delta}_{\boldsymbol{\lambda}_{dq}}(t) = 0$ (i.e., $\Delta_{\boldsymbol{\lambda}_{dq}}(t)$ is constant), which is only true at steady states because the disturbance term, defined by

$$\Delta_{\boldsymbol{\lambda}_{dq}}(t) := \boldsymbol{\lambda}_{dq}(t) (= \boldsymbol{f}(\boldsymbol{i}_{dq}(t))) - \boldsymbol{L}_{s,0} \boldsymbol{i}_{dq}(t), \tag{5}$$

is a function of the stator currents. Therefore, the flux linkage estimation cannot converge during transient states and even may have a large transient error when using an inaccurate nominal inductance matrix, as the nonzero $\dot{\Delta}_{\boldsymbol{\lambda}_{dq}}(t)$ term functions as a time-varying external effect.

III. Extended State Observer-based Flux Linkage Estimator (ESO-FLE)

This section presents ESO-FLE, which is an improved version of DOB-FLE with enhanced transient performance. The key idea is to assign non-zero dynamics for $\Delta_{\boldsymbol{\lambda}_{dq}}$ by introducing an extended state.

A. Extended State-Space Model

Extended states l_{dq} is added to the nonlinear disturbance dynamics as follows:

$$\begin{cases} \dot{\Delta}_{\boldsymbol{\lambda}_{dq}}(t) = \boldsymbol{l}_{dq}(t) \\ \dot{l}_{dq}(t) = 0. \end{cases} \tag{6}$$

The extended states are regarded as constant terms, thereby making the nonlinear disturbance term ramp signals with constant slopes. This model is more expressive than regarding the nonlinear disturbance term as constant.

A extended state-space model is obtained by replacing the nonlinear disturbance dynamics in (4) with (6):

$$\begin{cases} \dot{\boldsymbol{x}}(t) = \boldsymbol{A}(\omega_r) \boldsymbol{x}(t) + \boldsymbol{B} \boldsymbol{u}(t) \\ \boldsymbol{y}(t) = \boldsymbol{C} \boldsymbol{x}(t) \end{cases} \tag{7}$$

with

$$\boldsymbol{x} := \begin{bmatrix} \boldsymbol{\lambda}_{dq} & \Delta_{\boldsymbol{\lambda}_{dq}} & l_{dq} \end{bmatrix}^T,$$
$$\boldsymbol{A}(\omega_r) := \begin{bmatrix} -R_s {\boldsymbol{L}_{s,0}}^{-1} - \omega_r \boldsymbol{J} & R_s {\boldsymbol{L}_{s,0}}^{-1} & \boldsymbol{O}_{2\times2} \\ \boldsymbol{O}_{2\times2} & \boldsymbol{O}_{2\times2} & \boldsymbol{I}_2 \\ \boldsymbol{O}_{2\times2} & \boldsymbol{O}_{2\times2} & \boldsymbol{O}_{2\times2} \end{bmatrix},$$
$$\boldsymbol{B} := \begin{bmatrix} \boldsymbol{I}_2 \\ \boldsymbol{O}_{2\times2} \\ \boldsymbol{O}_{2\times2} \end{bmatrix}, \boldsymbol{C} := \begin{bmatrix} {\boldsymbol{L}_{s,0}}^{-1} & -{\boldsymbol{L}_{s,0}}^{-1} & \boldsymbol{O}_{2\times2} \end{bmatrix},$$

where $\boldsymbol{x}$ denotes the state, and, $\boldsymbol{A}(\omega_r)$, $\boldsymbol{B}$ and $\boldsymbol{C}$ represent the system, input and output matrices, respectively. To analyze

TABLE I
SPECIFICATIONS OF THE IPMSM DRIVE

Parameter	Value
Base speed	2000 RPM
Maximum torque	180 Nm
DC-link voltage	325 V
Maximum stator current	350 A
Rotor Inertia	0.1234 kg$\cdot m^2$
Number of pole pairs	8
Stator winding resistance (R_s)	10.9 mΩ

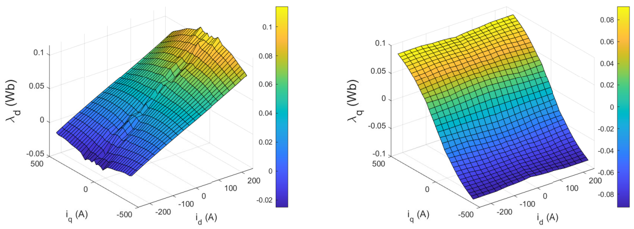

(a) (b)

Fig. 1. Nonlinear flux linkage maps of the IPMSM. (a) d-axis and (b) q-axis.

whether the states of system (7) are fully observable, the observability matrix is obtained by

$$\boldsymbol{\mathcal{O}}(\omega_r) = \begin{bmatrix} \boldsymbol{C} \\ \boldsymbol{C}\boldsymbol{A}(\omega_r) \\ \boldsymbol{C}\boldsymbol{A}(\omega_r)^2 \\ \boldsymbol{C}\boldsymbol{A}(\omega_r)^3 \end{bmatrix}, \tag{8}$$

which is evaluated using the first three rows of $\boldsymbol{\mathcal{O}}(\omega_r)$ for the simplicity. Consequently, the observability matrix has full rank (i.e., $\boldsymbol{\mathcal{O}}(\omega_r)$ = 6) if $\omega_r \neq 0$, and the state $\boldsymbol{x}$ is fully observable.

B. Extended State Observer Design

A linear extended state observer for the model (7) is designed as follows:

$$\begin{cases} \dot{\hat{\boldsymbol{x}}}(t) = \boldsymbol{A}(\omega_r)\hat{\boldsymbol{x}}(t) + \boldsymbol{B}\boldsymbol{u}(t) + \boldsymbol{F}(\boldsymbol{y}(t) - \hat{\boldsymbol{y}}(t)) \\ \hat{\boldsymbol{y}}(t) = \boldsymbol{C}\hat{\boldsymbol{x}}(t), \end{cases} \tag{9}$$

where $\hat{\boldsymbol{x}}$ and $\hat{\boldsymbol{y}}$ represent the estimates of $\boldsymbol{x}$, and $\boldsymbol{y}$ and $\boldsymbol{F}$ is the feedback gain matrix dependent on the the electrical rotor speed w_r. The estimation error dynamics is obtained by subtracting (9) from (7) as

$$\dot{\boldsymbol{e}}(t) = [\boldsymbol{A}(\omega_r) - \boldsymbol{F}\boldsymbol{C}]\,\boldsymbol{e}(t), \tag{10}$$

where $\boldsymbol{e} := \boldsymbol{x} - \hat{\boldsymbol{x}}$ denotes the estimation error. If the gain matrix $\boldsymbol{F}$ is designed to ensure that the matrix $\boldsymbol{A}(\omega_r) - \boldsymbol{F}\boldsymbol{C}$ has the desired stable eigenvector, the estimation error $\boldsymbol{e}(t)$ exponentially converges to zero. Note that DOB-FLE has the same structure as ESO-FLE except that the system matrix $\boldsymbol{A}(\omega_r)$ is different due to the use of different nonlinear disturbance dynamics.

IV. VALIDATION

The proposed ESO-FLE was validated using MATLAB/SIMULINK simulation, built based on the '`Three-phase PMSM Traction Drive`' example provided by MathWorks. A 35-kW IPMSM drive, whose specifications and flux linkage maps are listed in Table I and shown in Fig. 1, respectively, was controlled by finite control set MPC [17] to track the current references. A numerical reference generator presented in [18] was used to convert a torque command into the current references. The feedback gain matrix $\boldsymbol{F}$ was selected so that the eigenvalues of matrix $\boldsymbol{A}(\omega_r) - \boldsymbol{F}\boldsymbol{C}$ became 628 rad/s at a mechanical speed of 500 RPM.

The simulation validation consisted of two parts. In the first part (see Section IV-A), the performance of the proposed ESO-FLE was examined while controlling the torque ranging from -180 to 180 Nm within a mechanical speed range from 200 to 1300 RPM. The nominal inductance matrix is defined by the secant inductance values along the d-axis and q-axis at zero current, placed as diagonal elements, with all off-diagonal elements set to zero (i.e., $\boldsymbol{L}_{s,0} = \begin{bmatrix} 0.28 & 0 \\ 0 & 0.28 \end{bmatrix}$ mH). In the second part (see Section IV-B), ESO-FLE was compared with DOB-FLM, under the condition that a torque command increased from 0 to 180 Nm within 0.05 s at a mechanical speed of 500 RPM. The feedback gain matrix of DOB-FLE was also selected so that it had the same eigenvalues at 500 RPM as ESO-FLE. The nominal inductance matrix was set to $\boldsymbol{L}_{s,0} = \begin{bmatrix} 0.14 & 0 \\ 0 & 0.14 \end{bmatrix}$ mH, which is half of the value defined in the first part, for both ESO-FLE and DOB-FLE to simulate an adverse scenario.

A. Validation of the Proposed ESO-FLE

Figure 2 shows the flux linkage estimates, their estimation error $\boldsymbol{e}_\lambda := \boldsymbol{\lambda}_{dq} - \hat{\boldsymbol{\lambda}}_{dq}$, and the operating conditions for the proposed ESO-FLE. The flux linkage estimates closely tracked their true values under dynamic operating conditions across a wide operating range of torque and speed. The estimation error was nearly identical in both transient and steady states, suggesting that incorporating the extended state into the state-space model effectively enhanced the transient performance.

B. Comparison of ESO-FLE and DOB-DLE

Figure 3 shows the comparison results between ESO-FLE and DOB-FLE, demonstrating that ESO-FLE exhibits superior transient performance compared to DOB-FLE. This enhancement can be attributed to ESO-FLE's approach of treating the nonlinear disturbance term as time-varying ramp signals, unlike DOB-FLE which assumes these disturbances to be constant at zero.

Fig. 3b shows the estimation error norm $\|\boldsymbol{e}_\lambda\|$ between ESO-FLE and DOB-FLE, representing the quantitative estimation performance. It is evident that only the estimation error of ESO-FLE decreased during transient states. Consequently, it is demonstrated that the proposed method performs well in both steady and transient states even with inaccurate nominal inductance.

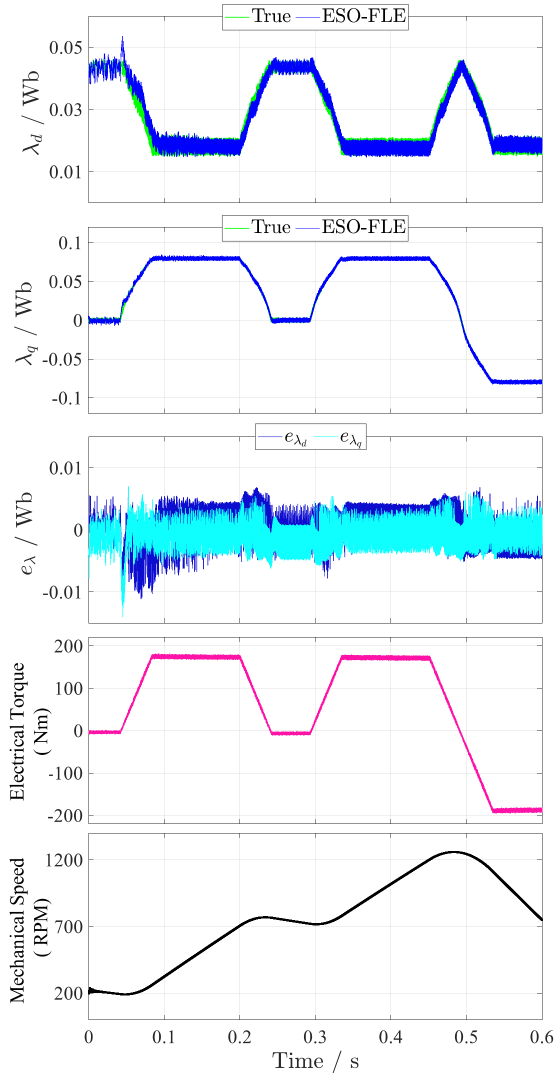

Fig. 2. Flux linkage estimates of the proposed ESO-FLE.

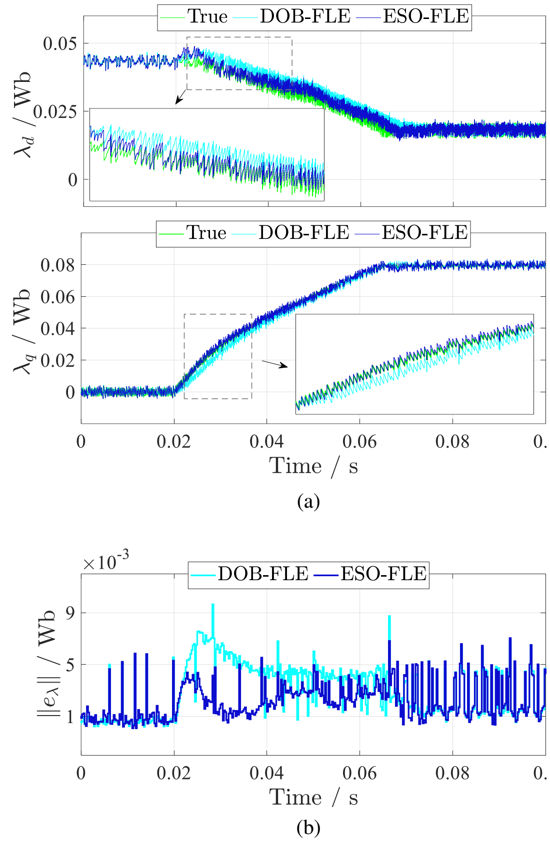

Fig. 3. Comparison of the proposed ESO-FLE and DOB-FLE. (a) Flux linkage estimates. (b) The corresponding estimation error norm $\|\boldsymbol{e}_\lambda\|$.

V. Conclusion

This paper introduced ESO-FLE, an enhanced version of DOB-FLE, with the latter recognized as the state-of-the-art method for flux linkage estimation. The main contribution was introducing extended states to accurately model the nonlinear flux linkage dynamics, treating the nonlinear disturbance term as time-varying ramp signals. This differed from DOB-FLE, which treats the nonlinear disturbance term as a constant. Simulation results using a 35 kW IPMSM drive demonstrated that ESO-FLE outperformed DOB-FLE in transient performance for flux linkage estimation under dynamic operating conditions. Future research will focus on experimental validation of the proposed method, with a particular emphasis on addressing non-ideal factors such as inverter nonlinearities.

References

[1] Antonello, Riccardo, et al. "Advanced current control of synchronous reluctance motors." *2017 IEEE 12th International Conference on Power Electronics and Drive Systems (PEDS).* IEEE, 2017.

[2] Brosch, Anian, Oliver Wallscheid, and Joachim Böcker. "Torque and inductances estimation for finite model predictive control of highly utilized permanent magnet synchronous motors." *IEEE Transactions on Industrial Informatics* 17.12 (2021): 8080-8091.

[3] Wendel, Sebastian, et al. "Flux linkage-based direct model predictive current control for synchronous machines." *IEEE Transactions on Power Electronics* 36.12 (2021): 14237-14256.

[4] Y. Inoue, S. Morimoto, and M. Sanada, "Examination and linearization of torque control system for direct torque controlled IPMSM," *IEEE Transactions on Industry Applications*, vol. 46, no. 1, pp. 159–166, 2009.

[5] X. Sun, Y. Zhang, G. Lei, Y. Guo and J. Zhu, "An Improved Dead-beat Predictive Stator Flux Control With Reduced-Order Disturbance Observer for In-Wheel PMSMs," *IEEE/ASME Transactions on Mechatronics*, vol. 27, no. 2, pp. 690-700, April 2022.

[6] E. Armando, R. I. Bojoi, P. Guglielmi, G. Pellegrino, and M. Pastorelli, "Experimental identification of the magnetic model of synchronous machines," *IEEE Transactions on Industry Applications*, vol. 49, no. 5, pp. 2116-2125, 2013.

[7] A. Choudhury, P. Pillay, and S. S. Williamson, "Modified stator flux estimation based direct torque controlled PMSM drive for hybrid electric vehicle," in *IECON 2012-38th Annual Conference on IEEE Industrial Electronics Society*, pp. 2965–2970, IEEE, 2012.

[8] A. Yoo and S.-K. Sul, "Design of flux observer robust to interior permanent-magnet synchronous motor flux variation," *IEEE Transactions on Industry Applications*, vol. 45, DOI 10.1109/tia.2009.2027516, no. 5, pp. 1670–1677, 2009.

[9] G. Feng, C. Lai, and N. C. Kar, "A novel current injection-based online parameter estimation method for PMSMs considering magnetic saturation," *IEEE Transactions on Magnetics*, vol. 52, no. 7, pp. 1–4, 2016.

[10] K. Liu and Z.-Q. Zhu, "Position offset-based parameter estimation for permanent magnet synchronous machines under variable speed control," *IEEE Transactions on Power Electronics*, vol. 30, no. 6, pp. 3438–3446, 2014.

[11] D. F. Laborda, D. D. Reigosa, D. Fernandez, K. Sasaki, T. Kato,´ and F. Briz, “Enhanced torque estimation in variable leakage flux PMSM combining high and low frequency signal injection,” *IEEE Transactions on Industry Applications*, vol. 59, no. 1, pp. 801-813, 2022

[12] S. Huang and Q. Zhang, “Stator flux sliding mode observer of permanent magnet synchronous motor based on effective flux,” in *2022 4th International Conference on Intelligent Control, Measurement and Signal Processing (ICMSP)*, DOI 10.1109/icmsp55950.2022.9859031. IEEE, Jul. 2022.

[13] Vyncke, T. J., Boel, R. K., Melkebeek, J. A. A. (2010, February). On extended kalman filters with augmented state vectors for the stator flux estimation in SPMSMs. In *2010 Twenty-Fifth Annual IEEE Applied Power Electronics Conference and Exposition (APEC)* (pp. 1711-1718). IEEE.

[14] Monzen, Niklas, Bernd Pfeifer, and Christoph M. Hackl. ”A simple disturbance observer for stator flux linkage estimation of nonlinear synchronous machines.” *2023 IEEE 32nd International Symposium on Industrial Electronics (ISIE)*. IEEE, 2023.

[15] Jang, Seunghoon, and Kyunghwan Choi. ”Stator Flux Linkage Estimation of Synchronous Machines Based on Integration Error Estimation for Improved Transient Performance.” *2023 62nd IEEE Conference on Decision and Control (CDC)*. IEEE, 2023.

[16] Su, Shih-Wei, Christoph M. Hackl, and Ralph Kennel. ”Analytical prototype functions for flux linkage approximation in synchronous machines.” *IEEE Open Journal of the Industrial Electronics Society* 3 (2022): 265-282.

[17] J. Rodriguez et al., “Predictive current control of a voltage source inverter,” *IEEE Transactions on Industrial Electronics*, vol. 54, no. 1, pp. 495-503, 2007.

[18] K. Choi, Y. Kim, K.-S. Kim, and S.-K. Kim, “Real-time optimal torque control of interior permanent magnet synchronous motors based on a numerical optimization technique,” *IEEE Transactions on Control Systems Technology*, vol. 29, no. 4, pp. 1815-1822, 2020.